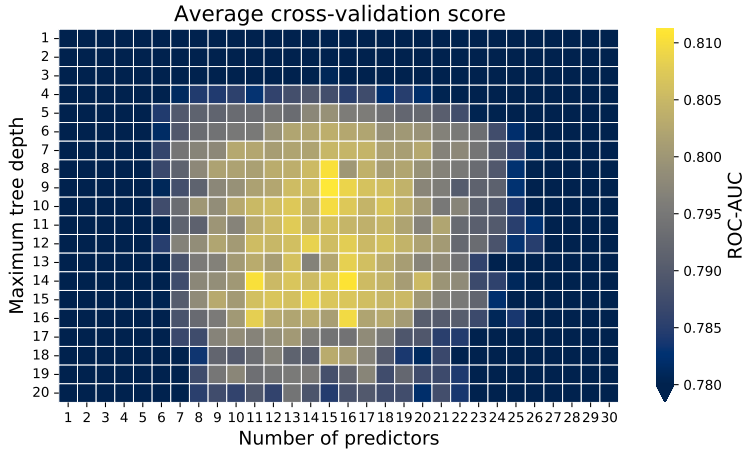

Figure S1: Average cross-validation (CV) ROC-AUC scores for all combinations of maximum tree depth and number of predictors.

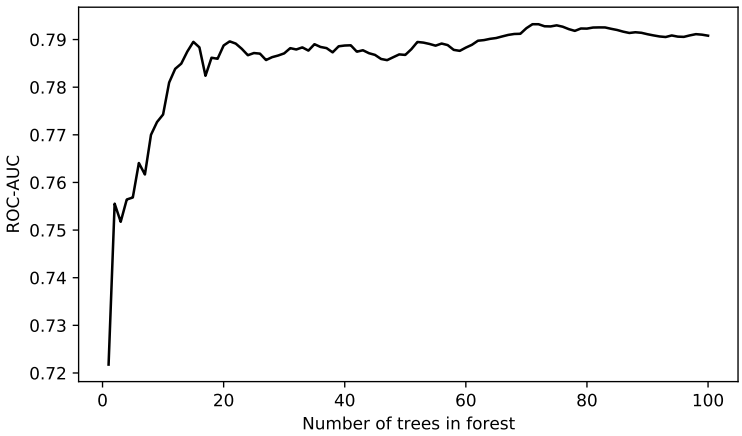

Figure S2: Stabilisation of test-set prediction score (ROC-AUC) for increasing number of trees, using the max tree depth and predictors of the data-driven model for Fennoscandia.

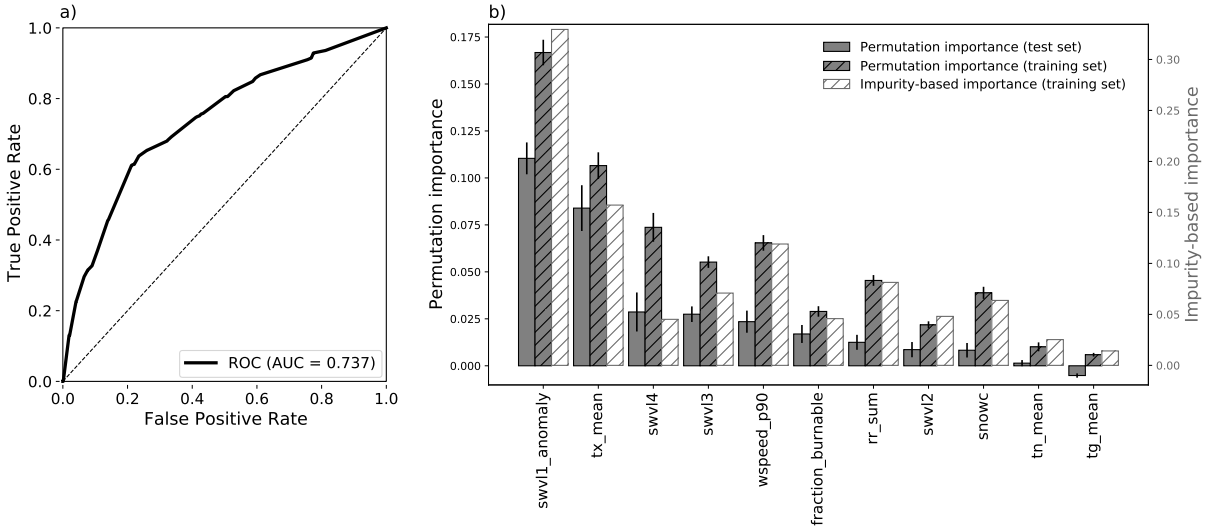

Figure S3: Results of a data-driven model trained in the same way as for the main analysis, but using a Decision Tree instead of a Random Forest machine learning algorithm: a) ROC curve and ROC-AUC score of test-set, and b) predictor importances as described in Fig. 6. The model had a maximum tree depth of 7 and 11 predictors.

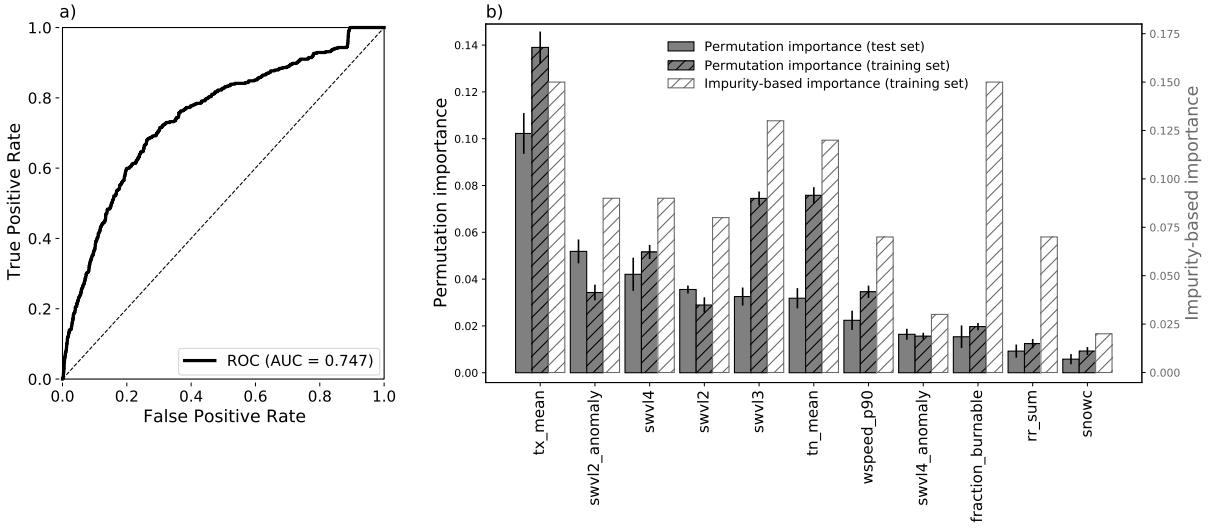

Figure S4: Results of a data-driven model trained in the same way as for the main analysis, but using AdaBoost with single splits instead of a Random Forest machine learning algorithm: a) ROC curve and ROC-AUC score of test-set, and b) predictor importances as described in Fig. 6. The model had 100 trees and 11 predictors.

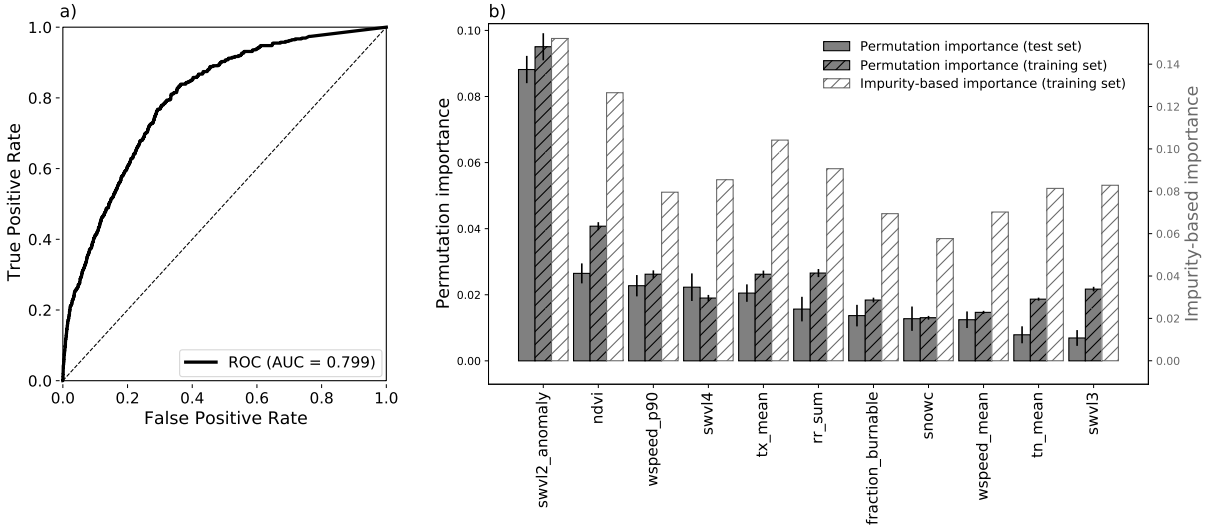

Figure S5: Results of a data-driven model trained in the same way as for the main analysis, but with NDVI included as a potential predictor: a) ROC curve and ROC-AUC score of test-set, and b) predictor importances as described in Fig. 6. The model had a maximum tree depth of 16 and 11 predictors.

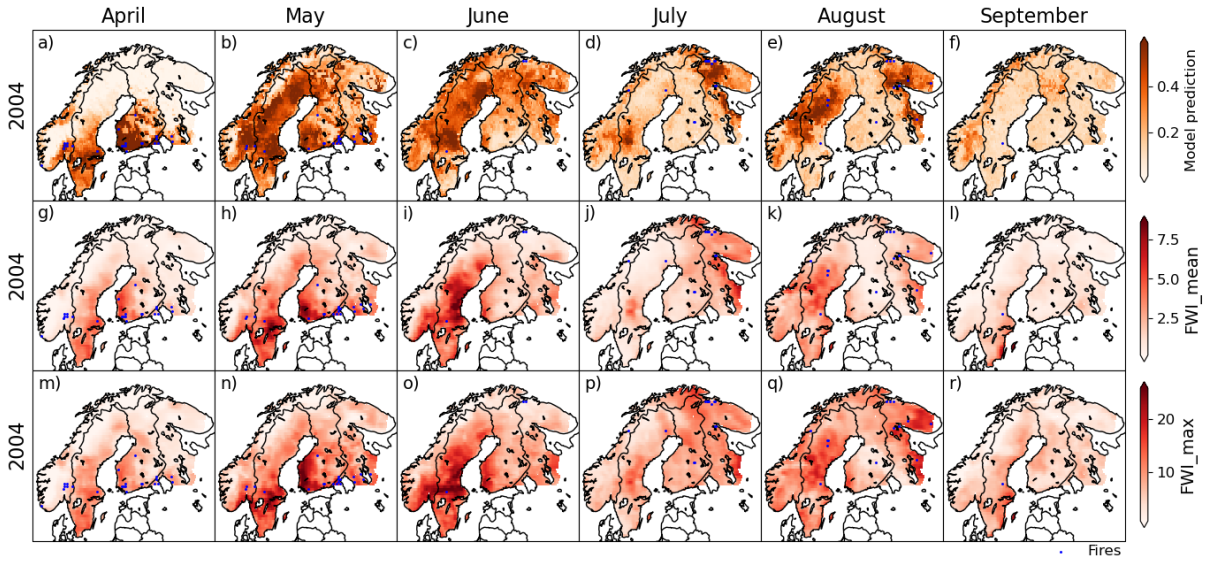

Figure S6: Fire danger probability maps for April–September 2004 using a)-f) the data-driven model predictions, g)-l) the FWI_mean, and m)-r) FWI_max. Blue markers show fire occurrences using the satellite-based fire occurrence dataset. Colour axes are truncated at the 5th and 95th percentile.

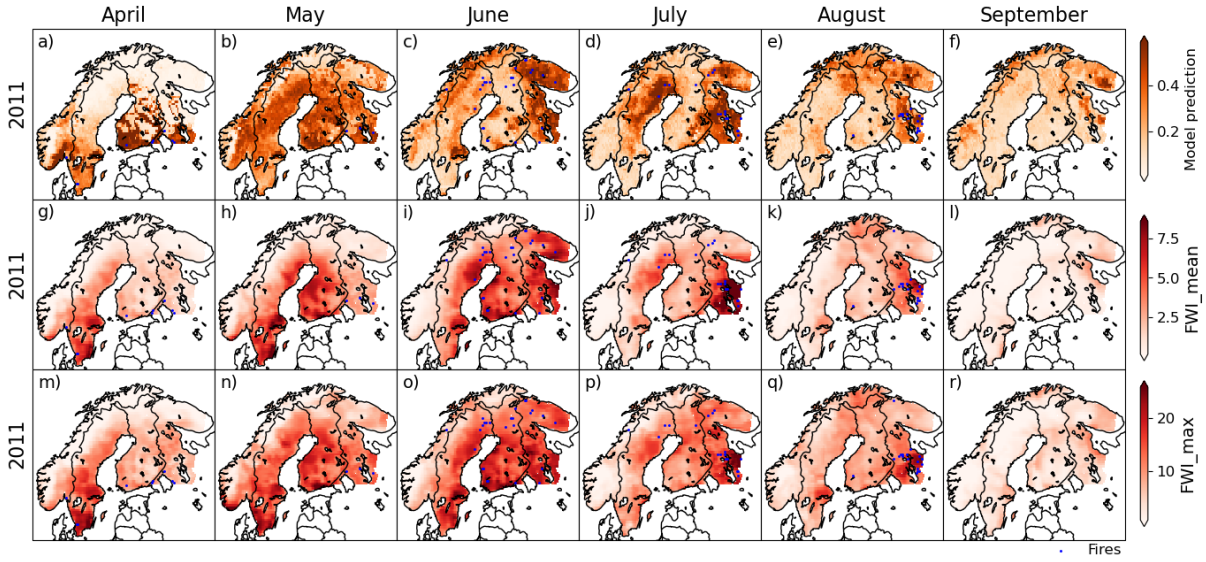

Figure S7: Fire danger probability maps for April–September 2011 using a)-f) the data-driven model predictions, g)-l) the FWI_mean, and m)-r) FWI_max. Blue markers show fire occurrences using the satellite-based fire occurrence dataset. Colour axes are truncated at the 5th and 95th percentile.

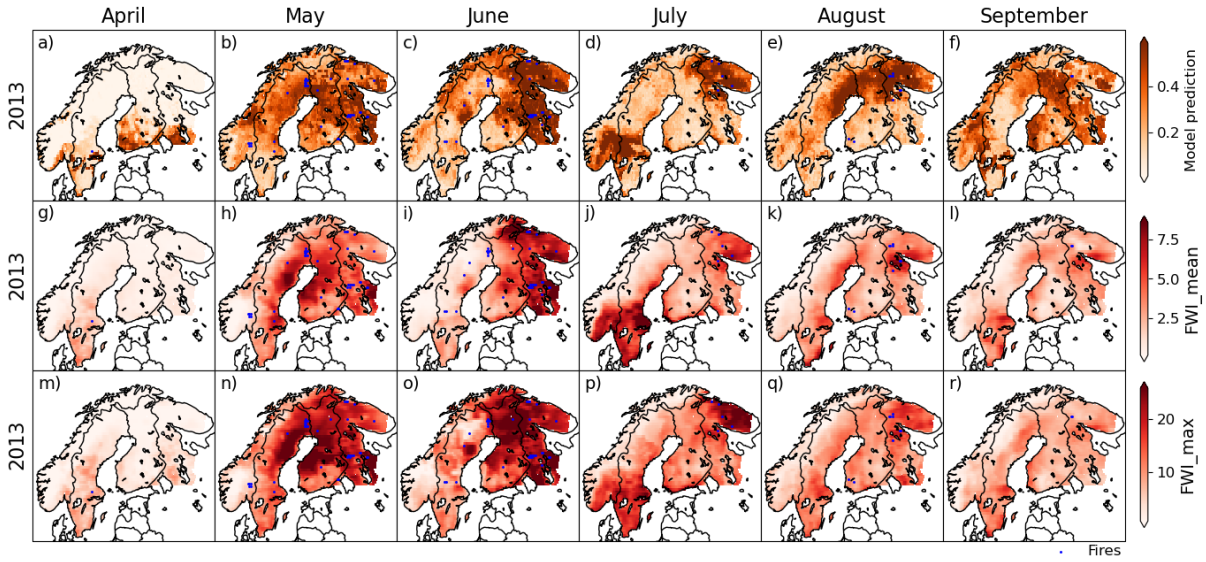

Figure S8: Fire danger probability maps for April–September 2013 using a)-f) the data-driven model predictions, g)-l) the FWI_mean, and m)-r) FWI_max. Blue markers show fire occurrences using the satellite-based fire occurrence dataset. Colour axes are truncated at the 5th and 95th percentile.

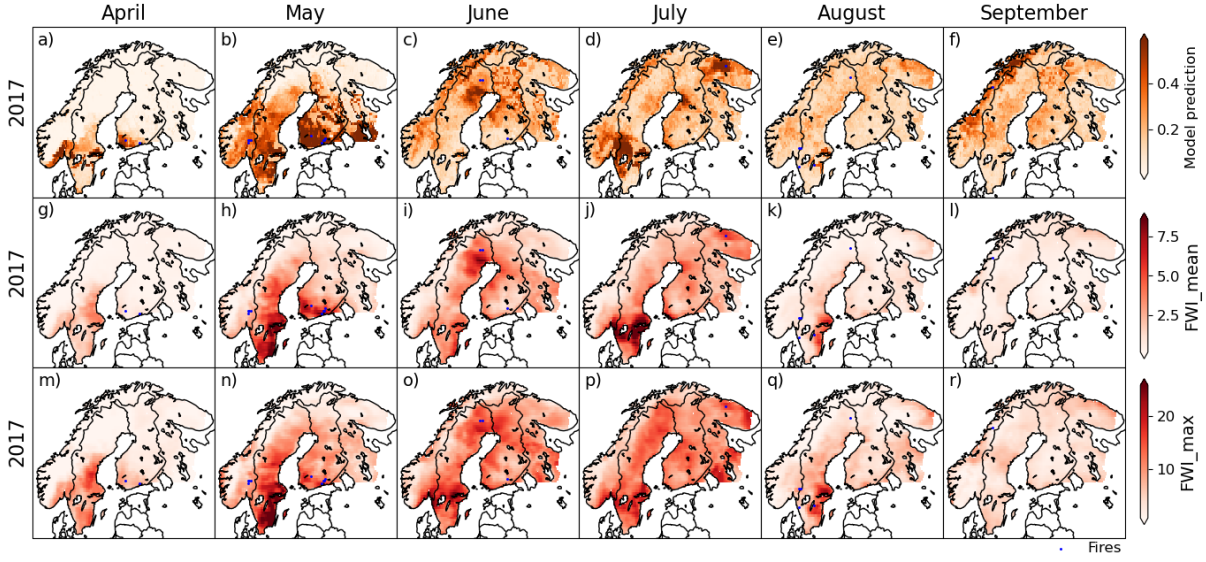

Figure S9: Fire danger probability maps for April–September 2017 using a)-f) the data-driven model predictions, g)-l) the FWI_mean, and m)-r) FWI_max. Blue markers show fire occurrences using the satellite-based fire occurrence dataset. Colour axes are truncated at the 5th and 95th percentile.

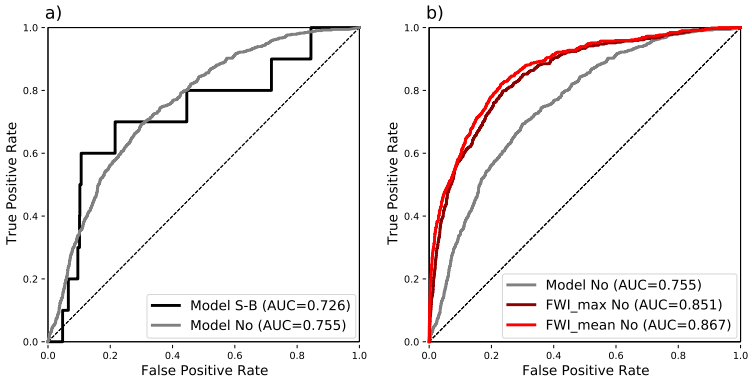

Figure S10: Test set ROC curve and ROC-AUC results for Norway: a) the data-driven model when predicting the satellite-based fire occurrence dataset (S-B) as compared to predicting the Norwegian fire occurrence dataset (No), and b) the data-driven model as compared to FWI_mean and FWI_max, all predicting the Norwegian fire occurrence dataset. Test set years are 2017 and 2018.

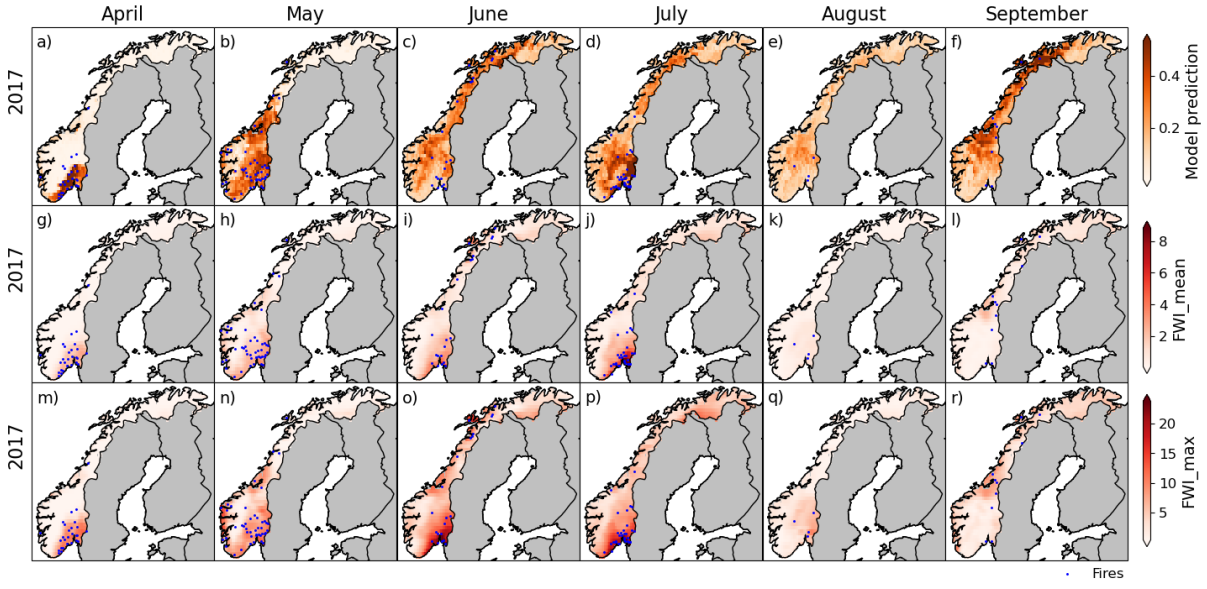

Figure S11: Fire danger probability maps for April–September 2017 using a)-f) the data-driven model predictions, g)-l) FWI_mean, and m)-r) FWI_max. Blue markers show fire occurrences using the Norwegian fire occurrence dataset. Colour axes are truncated at the 5th and 95th percentile.

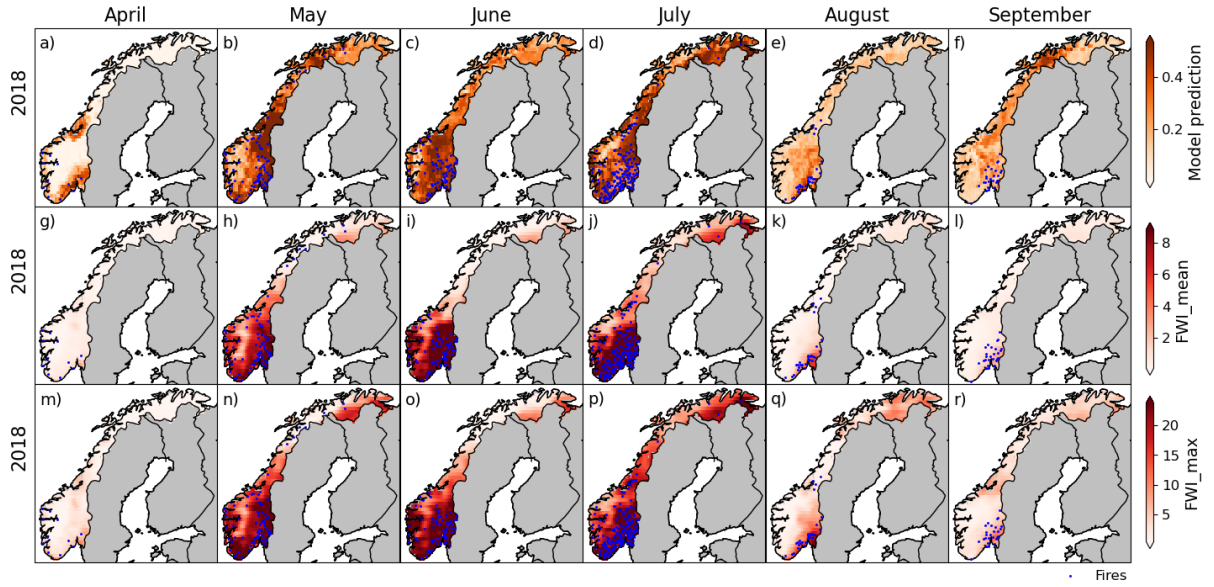

Figure S12: Fire danger probability maps for April–September 2018 using a)-f) the data-driven model predictions, g)-l) FWI_mean, and m)-r) FWI_max. Blue markers show fire occurrences using the Norwegian fire occurrence dataset. Colour axes are truncated at the 5th and 95th percentile.

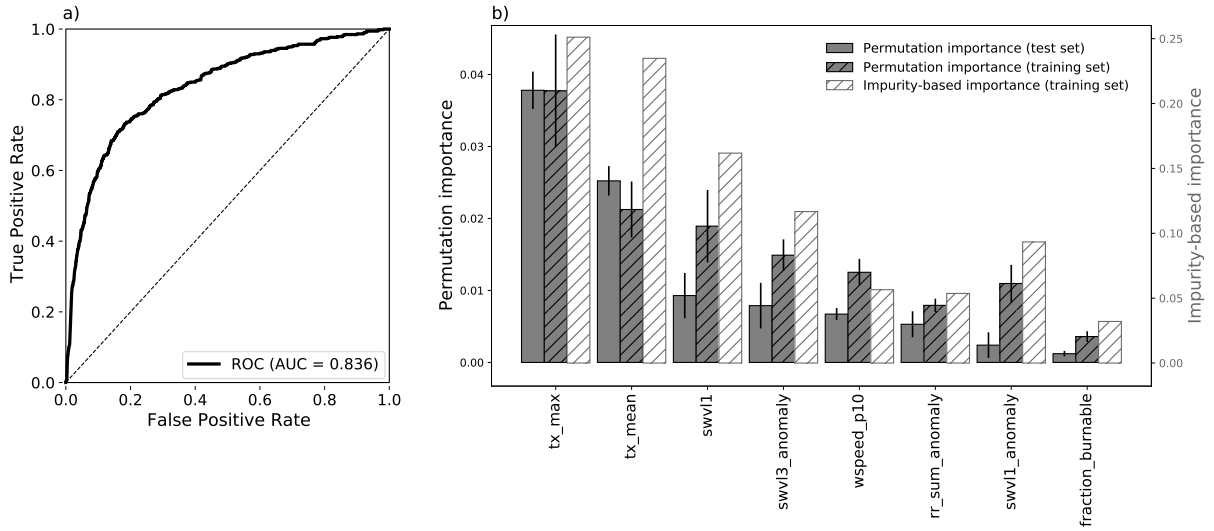

Figure S13: Results of the model trained on the Norwegian fire occurrence dataset: a) ROC curve and ROC-AUC score of test-set, and b) predictor importances as described in Fig. 6. Test set years are 2017 and 2018, and training set years are 2016 and 2019. The final model had a maximum tree depth of 2 and 8 predictors.